Global and Stochastic Analysis
Vol. 12 No. 1 (January, 2025)

Received: 06th July 2024 **Revised: 14th August 2024** **Accepted: 30th August 2024**

INFLUENCE OF VISCOUS DISSIPATION AND THERMAL RADIATION ON THE HEAT AND MASS TRANSFER CHARACTERISTICS OF THE MHD FLOW OF CASSON FLUID SQUEEZED IN A CHANNEL: A SEMI-ANALYTICAL APPROACH

PAREEKSHITH G. BHAT, NITYANAND P. PAI, DEVAKI B.,
AND SAMPATH KUMAR V. S.*

Abstract. The fundamental interaction that govern the fluid behaviour is the basis for the intricate relationship between fluid mechanics and chemistry. Further, the fluids, in general, exhibit dynamic properties that directly impact the chemical composition and molecular forces. The current study aims to analyse theoretically, the impact of viscous dissipation and thermal radiation on the of heat and mass transfer characteristics of the MHD flow of Casson fluid that is squeezed between a pair of plates placed parallel to each other. To achieve an approximate analytical solution to this problem by homotopy perturbation method (HPM), the fundamental equations that govern the flow, energy and chemical reaction are converted into non-linear ordinary differential equations (ODEs) with the help of similarity transformation. In the current analysis, the influence of various physical parameters on the velocity profile, temporal field, and concentration distribution curve are presented graphically. Further, in order to compare the results obtained by the HPM, a well-established numerical method, the classical finite difference method (FDM), is adopted. The numerical values of the magnitude of coefficient of skin friction, and heat and mass transfer rates obtained by the HPM are tabulated. Furthermore, the obtained semi-analytical solutions are compared with that of the solution obtained by the classical FDM. From the tables it is clear that the results obtained by both techniques are in good agreement. It is also noted that an increase in the radiation parameter is responsible for the retardation of the temporal profile, whereas it elevates the concentration field.

1. Introduction

The intricate relation between fluid mechanics and chemistry lies in the fundamental interaction that govern the fluid behaviour. Generally fluids exhibit dynamic properties that are influenced by the chemical composition and molecular forces. Understanding fluid flow, necessitates an appreciation of the underlying molecular interactions, delving into the realms of thermodynamics and molecular

2000 *Mathematics Subject Classification.* 34B15;76D05.
Key words and phrases. MHD, similarity transformations, heat transfer, mass transfer, homotopy perturbation method, finite difference method.

kinetics. Chemistry contributes to the comprehension of fluid properties, highlighting the interplay of molecular structures that dictate viscosity, density, and other critical fluid characteristics. Thus, the synergy between fluid mechanics and chemistry forms the basis for unravelling the intricacies of the fluid behaviour.

The study of fluid flow between a pair of plates placed parallel to one another is of great significance in fluid mechanics, owing to its wide-ranging applications across various scientific and industrial domains. The flow of fluids between plates placed parallelly has been a well-established field of chemical engineering that is commonly employed in heat exchanger, thin film coating and micro-fluidics. Micro-fluidics involves the flow of fluids through narrow channels between parallel plates for lab-on-a-chip devices, which have emerged as highly effective tools for chemical analysis and drug discovery. Heat exchangers benefit from parallel plates as they significantly increase the surface area available for heat transfer, resulting in a more efficient process. Moreover, fluid flow between parallel plates are also utilized in thin film coating to ensure a uniform and even distribution of liquid or gas on a substrate, which is a critical aspect of this production process.

The application of squeezing fluid flow through a channel of parallel plates has revolutionised the field of chemistry, especially in micro-fluidic devices for chemical analysis and synthesis. These devices can operate on a small scale, delivering precise volumes of reagents to carry out chemical reactions. The thin films created through this technique are used in surface chemistry for studying surface reactions, synthesising new materials, and developing coatings for various applications. Additionally, this technique is used in electrochemistry to study the behaviour of ions and molecules in solution. Researchers use it to manipulate the flow of ions and molecules, control their concentration, and study their behaviour in real-time, which has enabled the development of new materials for energy storage and environmental remediation.

C.Y. Wang [1] theoretically analysed the fluid flow that is being squeezed between two plates with a novel set of similarity transformations. P.S. Gupta and A.S. Gupta [2] theoretically investigated the unsteady fluid flow between a pair plates that are symmetrically approaching or receding from each other. Further, they found that as the distance between the two plates varied as the square root of a linear function of time, the similarity solution existed. P. Singh et al. [3] numerically analysed the flow between two symmetrically approaching or receding parallel plates by transforming the fundamental Navier-Stokes equations into ordinary differential equations by employing similarity transformations.

Q.K. Ghori et al. [4] theoretically examined the effects of fluid inertia in the study of axisymmetric viscous flow caused due to two parallel massive plates moving slowly towards one another. Several other researchers have significantly contributed in the advancement of this field [5, 6]. Altogether, the fluid flow being squeezed between a pair of parallel plates is a powerful tool in the field of chemistry and has enabled researchers to carry out complex reactions with high precision, synthesise new materials, and study the behaviour of ions and molecules in solution.

The study of magnetohydrodynamics (MHD) fluid flow squeezed between parallel plates has several useful applications in chemistry. One of the significant

applications is the exploration of electro-kinetic phenomena, where an externally applied electric and magnetic field influence the movement of charged particles in a fluid. Further, this type of fluid flow can be employed to develop innovative micro-fluidic devices for chemical analysis, synthesis, and separation. The flow generated between the parallel plates can enhance mass transfer between the fluid and the solid surface, boost reaction kinetics, and increase mixing efficiency. Moreover, MHD flow between parallel plates can also be used to create pumps and valves for micro-fluidic devices, generating high flow rates without the need for moving parts. This makes them ideal for handling small volumes of fluids during chemical synthesis and analysis. Another useful application of MHD fluid flow through a channel of parallel plates is the manipulation and separation of magnetic particles, which have become increasingly important in various chemical and biological processes.

A.M. Siddiqui et al. [7] theoretically examined the unsteady MHD flow viscous fluid through a two-dimensional channel of two infinitely parallel plates that are symmetrically approaching each other causing the squeezing flow. Erik Sweet et al. [8] theoretically analysed the unsteady viscous MHD fluid flow between a pair of moving parallel plates that cause a squeezing flow. Further, they have showed that the strength of the applied magnetic field and the density strongly influences the flow of the fluid. Various other researchers have also contributed in the study of MHD flow in the recent past [9, 10, 11, 12]. Overall, MHD flow of fluid being squeezed between parallel plates offers a promising avenue for developing innovative solutions in the field of chemistry, and ongoing research is expected to lead to even more creative applications in the future.

Exploring the sequel of thermal radiation on flow of MHD fluid that is squeezed between plates placed parallel to one another is a fascinating and challenging area of research that requires a comprehensive understanding of fluid dynamics and heat transfer principles. By investigating the behaviour of fluids in such conditions, researchers can gain valuable insights into the underlying physical phenomena and develop advanced engineering solutions. The presence of magnetic fields and confined geometry can have a crucial influence on the flow dynamics and characteristics of heat transfer, making it an exciting area for researchers. With the help of advanced numerical and analytical tools, researchers can model and simulate these complex systems, leading to a better understanding of the underlying physics and potential applications in various industries.

H. M. Duwairi et al. [13] examined the unsteady squeezing and extrusion of a viscous fluid flow between plates placed parallel to each other of constant temperature. A. S. Dogonchi [14] theoretically analysed the flow and heat characteristics of an unsteady MHD nanofluid between parallel plates in the presence of thermal radiation. The influence of non-linear thermal radiation on unsteady MHD fluid flow between a pair of parallel plates was theoretically analysed by M. Sathish Kumar et al. [15]. Further, numerous other researchers have contributed in the development of repercussion of thermal radiation on the heat transfer and its applications [16, 17, 18].

The field of chemical engineering is continuously exploring the potential of the fluid flow between parallel plates, as it provides a conducive environment for the

occurrence of chemical reactions and mass transport of chemical species. This phenomenon is widely studied to understand the intricacies of diffusion and reaction kinetics. The thin films formed by chemical reactions in this system offer a plethora of opportunities to create functional coatings that can be immensely beneficial in various industries. Therefore, this area of research holds great significance and has the potential to revolutionise numerous industrial processes.

The mass transfer of MHD fluid flow squeezed between plates placed parallelly with thermal radiation has a broad scope in the field of chemistry. This technique can greatly aid in studying the transport phenomena during chemical reactions, leading to a better understanding of reaction rates and product yields. Moreover, it can help in designing chemical reactors and optimizing heat and mass transfer processes, which can result in more efficient and cost-effective manufacturing processes. The effect of magnetic fields and thermal radiation on fluid behaviour can be better understood with this method, allowing for the development of more advanced chemical engineering solutions.

M. Mustafa et al. [19] theoretically analysed the heat transfer and mass transfer characteristics in a viscous fluid flow squeezed between a pair of parallel plates. The heat transfer and mass transfer characteristics was theoretically analysed by Abdul-Sattar J. Al-Saif and Assma J. Harfash [20] adopting perturbation-iteration algorithm. Further, the authors employed similarity transformation to transform the governing equations into ordinary differential equations so as to analyse the repercussion of various physical parameters on the velocity, temperature and concentration profile in addition to Sherwood number, skin friction coefficient and Nusselt number. Numerous other researchers have also contributed in the development of this field in the recent past [21, 22, 24, 23, 25, 26, 27]. Overall, the mass transfer of MHD fluid flow squeezed between plates placed parallel to each other with thermal radiation is a constructive tool in the advancement of chemical research and engineering applications.

Casson fluids are a type of non-Newtonian fluids that have become popular due to their unique rheological properties, which make them useful in various industrial applications. These fluids exhibit a yield stress, meaning they do not flow until a specific stress level is applied to them. Once this stress level is surpassed, they show a linear relationship between the shear rate and shear stress. They are commonly used in the oil and gas industry as drilling muds to lubricate the drill bit and carry rock cuttings. Casson fluids are also used in several food products, such as sauces, dressings, and dairy products, to provide a smooth, creamy texture and prevent separation. Besides, they are used in pharmaceuticals, cosmetics, paints, and coatings, to regulate viscosity, enhance flow properties, and provide a smooth, stable consistency.

The MHD Casson fluid flow squeezed between a pair of parallel plates presents multiple opportunities for practical application. For instance, it can aid in accurately modelling the flow of blood in narrow arteries or veins, or in understanding the lubrication of metalworking fluids during industrial processes. The Casson fluid model is particularly valuable in characterising non-Newtonian fluids with yield stress, enabling researchers to gain a better understanding of their intricate flow behaviour under different conditions. By leveraging this knowledge, engineers

and scientists can design better processes that optimise efficiency, reduce waste, and improve safety and performance in various applications.

In the recent years, the flow of MHD Casson fluid with thermal radiation has been gaining a prominent interest due to its application in cancer treatment. This innovative approach has the potential to revolutionise cancer treatment by combining the principles of fluid dynamics, magnetic fields, and thermal radiation. By utilising this approach, cancer cells can be targeted and destroyed with minimal damage to healthy cells, thus reducing the side effects associated with traditional cancer treatments. Although this technique is still in its early stages, it has shown promising results in laboratory studies. With further research and development, flow of MHD Casson fluid with thermal radiation could become a highly effective and targeted form of cancer treatment, offering hope to millions of people affected by cancer.

U. Khan et al. [28] analysed the squeezing flow of Casson fluid by imposing similarity transformations on the conservation laws that govern the fluid flow so as to obtain a non-linear ordinary differential equation governing the flow. Further, U. Khan et al. [29] extended it to theoretically analysed the transfer of heat in the Casson fluid flow squeezed between a pair of parallel plates. Various other researchers have analysed the Casson fluid flow squeezed between a pair of parallel plates in the recent past [30, 31, 32, 33].

Formulating and solving the governing equations with specific boundary conditions is crucial once the physical problem is identified. However, the non-linearity involved in the fundamental equations governing the flow makes it cumbersome to solve using known analytical methods. As a result, researchers rely on numerical methods to obtain an approximate numerical solution. Despite its effectiveness, numerical methods present several difficulties, prompting modern researchers to explore semi-analytical methods. Among these methods, HPM shows great potential in solving non-linear differential equations with high accuracy. Proposed by Ji-Huan He [34] in 1999, HPM is one of the semi-analytical method with wide range of applicability and higher accuracy. Further, he suggested a method for dealing with non-linear problems using this technique, and also demonstrated the efficiency and practicality of HPM [35, 36]. Several other researchers have implemented the elegant and powerful technique, HPM to solve non-linear differential equations arising in various scenarios in the recent days [37, 38, 39, 40].

This study aims to analyse the heat transfer and mass transfer characteristics on the flow of MHD Casson fluid between parallel plates in the presence of thermal radiation. To achieve accurate results, a semi-analytical technique, HPM, is adopted. HPM is considered to be advantageous in comparison to other mathematical techniques in terms of accuracy and the ability to obtain solutions for a large number of expansions using a single computer program. In addition, HPM is a highly stable method that provides insight into the analytic structure of the solution function [41]. The computational effort required for the method is minimal, making it an efficient tool for obtaining accurate results. The classical finite difference method yields a numerical solution which is used to compare the solution obtained by HPM.

2. Mathematical Formulation

Consider a two-dimensional unsteady MHD flow of Casson fluid between two plates placed parallel to each other at a distance $z = \pm d(1-\alpha t)^{(\frac{1}{2})} = \pm h(t)$ apart, where d is the initial position at time $t = 0$. Let T_1 and T_2 being the temperatures of the bottom and top plates respectively, and C_1 and C_2 are the concentrations of the two plates. Here, $\alpha > 0$ corresponds to the squeezing of the plates until they touch each other, whereas $\alpha < 0$ for plates dilating from each other as depicted in Figure 1.

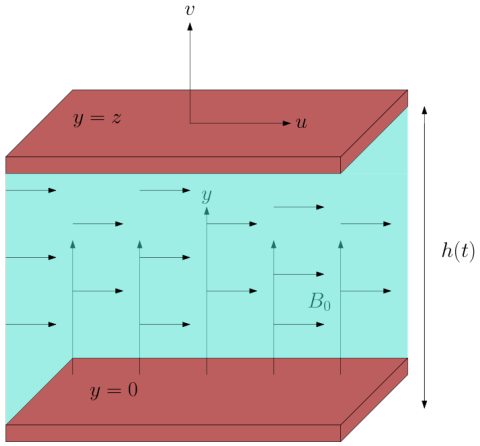

FIGURE 1. Geometry of the Flow

The equations governing the flow, energy and chemical reaction are thus given by

$$\frac{\partial u}{\partial x} + \frac{\partial v}{\partial y} = 0, \tag{2.1}$$

$$\frac{\partial u}{\partial t} + u\frac{\partial u}{\partial x} + v\frac{\partial u}{\partial y} = -\frac{1}{\rho}\frac{\partial p}{\partial x} + \nu\left(1+\frac{1}{\gamma}\right)\left(2\frac{\partial^2 u}{\partial x^2} + \frac{\partial^2 u}{\partial y^2} + \frac{\partial^2 u}{\partial x \partial y}\right), \tag{2.2}$$

$$\frac{\partial v}{\partial t} + u\frac{\partial v}{\partial x} + v\frac{\partial v}{\partial y} = -\frac{1}{\rho}\frac{\partial p}{\partial y} + \nu\left(1+\frac{1}{\gamma}\right)\left(\frac{\partial^2 v}{\partial x^2} + 2\frac{\partial^2 v}{\partial y^2} + \frac{\partial^2 v}{\partial x \partial y}\right), \tag{2.3}$$

$$\frac{\partial T}{\partial t} + u\frac{\partial T}{\partial x} + v\frac{\partial T}{\partial y} = \frac{k}{\rho C_p}\left(\frac{\partial^2 T}{\partial x^2} + \frac{\partial^2 T}{\partial y^2}\right) + \frac{\nu}{C_p}\left(1+\frac{1}{\gamma}\right)\left(\frac{\partial u}{\partial y}\right)^2, \tag{2.4}$$

$$\frac{\partial C}{\partial t} + u\frac{\partial C}{\partial x} + v\frac{\partial C}{\partial y} = D_B\left(\frac{\partial^2 C}{\partial x^2} + \frac{\partial^2 C}{\partial y^2}\right) + \frac{D_T}{T_1}\left(\frac{\partial^2 T}{\partial x^2} + \frac{\partial^2 T}{\partial y^2}\right) - k_1(C - C_1), \tag{2.5}$$

where p is the pressure, x and y-directional velocities are respectively given by u and v, ν the fluid's kinematic viscosity and $\gamma = \mu_B\sqrt{\frac{2\pi_c}{p_y}}$ is the Casson fluid parameter. The system temperature, specific heat and fluid's thermal conductivity

are respectively denoted by T, C_P and k. Further, the chemical concentration of the system, Brownian motion coefficient, thermophoresis diffusion coefficient and first-order chemical reaction rate are denoted by C, D_B, D_T and k_1 respectively.

By the Rosseland approximations for radiation [42],

$$q_{rad} = -\frac{4\sigma^*}{3k^*}\frac{dT^4}{dy}. \tag{2.6}$$

Here, k^* denote the coefficient of mean absorption and σ^* represent the Stefan-Boltzmann constant. Further, by employing Taylor's series expansion around T_1,

$$T^4 \cong 4T_1^3T - 3T_1^4. \tag{2.7}$$

The boundary conditions to the considered problem are

$$\frac{\partial u}{\partial y} = 0, \qquad v = 0, \qquad T = T_1, \;\; C = C_1 \;\; at \;\; y = 0. \tag{2.8}$$

$$u = 0, \quad v = v_w = \frac{dh}{dt}, \quad T = T_2, \;\; C = C_2 \;\; at \;\; y = z. \tag{2.9}$$

By introducing the following similarity transformations in the considered problem,

$$\eta = \frac{y}{d\,(1-\alpha t)^{\frac{1}{2}}}, \tag{2.10}$$

$$u = \frac{\alpha x}{[2\,(1-\alpha t)]}F'(\eta), \tag{2.11}$$

$$v = \frac{-\alpha d}{\left[2\,(1-\alpha t)^{\frac{1}{2}}\right]}F(\eta), \tag{2.12}$$

$$G = \frac{T-T_1}{T_2-T_1}, \tag{2.13}$$

$$H = \frac{C-C_1}{C_2-C_1}, \tag{2.14}$$

the governing equations transform into

$$\left(1+\frac{1}{\gamma}\right)F^{iv}(\eta) - S[\eta F'''(\eta) + 3F''(\eta) + F'(\eta)F''(\eta) - F(\eta)F'''(\eta)] - M^2F''(\eta) = 0, \tag{2.15}$$

$$\left(1+\frac{4}{3}Rd\right)G''(\eta) - SPr[\eta G'(\eta) - F(\eta)G'(\eta)] + \left(1+\frac{1}{\gamma}\right)EcPr(F''(\eta))^2 = 0, \tag{2.16}$$

$$H''(\eta) + \frac{N_T}{N_B}G''(\eta) - ScS[\eta H'(\eta) - F(\eta)H'(\eta)] - KrScH(\eta) = 0, \tag{2.17}$$

The relevant boundary conditions are reduced into

$$F(\eta) = 0, \quad F''(\eta) = 0, \quad G(\eta) = 0, \; H(\eta) = 0 \; at \; \eta = 0, \tag{2.18}$$

$$F(\eta) = 1, \quad F'(\eta) = 0, \quad G(\eta) = 1, \; H(\eta) = 1 \; at \; \eta = 1. \tag{2.19}$$

3. Method of Solution

The Eqs. (2.15 - 2.17) with boundary conditions Eqs. (2.18, 2.19) are achieved by employing similarity transformations to the governing equations. The equations so obtained are non-linear in nature and solution to these equations using analytical methods is difficult with the existing knowledge. Thus, an approximate solution to the problem is obtained by numerical techniques. To subduer the challenges encountered in the two techniques, in addition to obtain a more approximate solution, researchers proposed the concept of semi-analytical method. To obtain an approximate analytical solution, the considered problem is approached by a very effective semi-analytical method, HPM. Further, to compare the solution so obtained by HPM, the classical FDM method is adopted to obtain the numerical solution to the problem. Here, a non-linear differential equation of order four representing the flow and two non-linear differential equations of order two respectively representing energy and chemical reaction are approached by HPM and FDM.

3.1. Homotopy Perturbation Method. The combination of the classical perturbation methodology with the theory of homotopy in topology is the HPM. Ji-Huan He [34] was the first to introduce this method in 1998. The present study employs HPM to obtain an approximate analytic solution to the considered problem. In HPM, the non-linear differential equation is generally expressed as the sum of a linear and a non-linear term. Further, a homotopy equation is constructed with the help of homotopy concept in topology. Finally, by adopting the classical perturbation methodology, an approximate analytic solution is obtained. Thus, the obtained non-linear ordinary differential equations are analysed by adopting HPM for system of equations.

Let the differential operators acting on the unknown function $g(\eta)$ be denoted by D_1, D_2 and D_3 with $g_1(\eta)$, $g_2(\eta)$ and $g_3(\eta)$ representing the three known functions. Thus, the ODEs representing the flow, energy and chemical equations considered problem can be generally expressed as

$$D_i[g(\eta)] - g_i(\eta) = 0. \tag{3.1}$$

Generally, D_is, the differential operator in HPM are expressed as a sum of one linear and remaining part, that is

$$D_i = L_i + R_i, \tag{3.2}$$

where the linear part of D_i is denoted by L_i and the other part by R_i.

Hence, by a wise choice of L_is and v_0s from the ODEs and boundary conditions specified in Eq. (2.15) - Eq. (2.17) and Eq. (2.18) and Eq. (2.19) respectively, the homotopy equation for Eq. (3.1) is constructed as mentioned below,

$$H_i(\xi_i, p) = (1-p)[L_i(\xi_i, p) - L_i(v_0(\eta))] + p[D_i(\xi_i, p) - g_i(\xi)] = 0, \tag{3.3}$$

where $i = 1, 2, 3$.

Assuming the solution of Eq. (3.3) in terms of power series,

$$\xi(\eta, p) = \sum_{n=0}^{\infty} p^n g_n(\eta). \tag{3.4}$$

when $p = 1$, Eq. (3.4)reduces the solution to the considered problem.

The initial four solutions to the ODEs by employing the above mentioned scheme as are given below:

$$F_0(\eta) = \frac{3\eta - \eta^3}{2}$$

$$G_0(\eta) = \eta$$

$$H_0(\eta) = \eta$$

$$\begin{aligned} F_1(\eta) = \frac{1}{280(\gamma+1)}(&-7\gamma M^2\eta^5 + 14\gamma M^2\eta^3 - 7\gamma M^2\eta \\ &+\gamma S\eta^7 - 28\gamma S\eta^5 + 53\gamma S\eta^3 - 26\gamma S\eta) \end{aligned}$$

$$\begin{aligned} G_1(\eta) = \frac{Pr}{40\gamma(4Rd+3)}(&-90\gamma Ec\eta^4 - 90Ec\eta^4 + 90\gamma Ec\eta \\ &+90Ec\eta + 3\gamma S\eta^5 - 10\gamma S\eta^3 + 7\gamma S\eta) \end{aligned}$$

$$H_1(\eta) = \frac{3SSc\eta^5 - 10SSc\eta^3 + 7SSc\eta + 20Sc\eta^3 Kr - 20Sc\eta Kr}{120}$$

$$\begin{aligned} F_2(\eta) = -\frac{\gamma^2}{7761600(\gamma+1)^2}(&4620M^4\eta^7 - 19404M^4\eta^5 \\ &+24948M^4\eta^3 - 10164M^4\eta - 1155M^2S\eta^9 + 37884M^2S\eta^7 \\ &-151074M^2S\eta^5 + 193116M^2S\eta^3 - 78771M^2S\eta \\ &-84S^2\eta^{11} - 3850S^2\eta^9 + 76428S^2\eta^7 \\ &-293832S^2\eta^5 + 374200S^2\eta^3 - 152862S^2\eta) \end{aligned}$$

$$\begin{aligned} G_2(\eta) = \frac{1}{67200(4Rd+3)^2\gamma(\gamma+1)}(&525Pr^2S^2\gamma^2\eta^9 - 30PrS^2\gamma^2\eta^9 \\ &-40PrRdS^2\gamma^2\eta^9 + 525Pr^2S^2\gamma\eta^9 - 16200EcPr^2S\gamma^2\eta^8 \\ &+9720EcPrS\gamma^2\eta^8 + 12960EcPrRdS\gamma^2\eta^8 - 16200EcPr^2S\eta^8 \\ &-32400EcPr^2S\gamma\eta^8 + 9720EcPrS\gamma\eta^8 + 12960EcPrRdS\gamma\eta^8 \\ &-2700Pr^2S^2\gamma^2\eta^7 + 1440PrS^2\gamma^2\eta^7 + 1920PrRdS^2\gamma^2\eta^7 + \cdots) \end{aligned}$$

$$\begin{aligned} H_2(\eta) = \frac{1}{201600N_B(4Rd+3)\gamma(\gamma+1)}(&525N_BS^2Sc^2\gamma^2\eta^9 \\ &+700N_BRdS^2Sc^2\gamma^2\eta^9 - 30N_BS^2Sc\gamma^2\eta^9 - 40N_BRdS^2Sc\gamma^2\eta^9 \\ &+525N_BS^2Sc^2\gamma\eta^9 + 700N_BRdS^2Sc^2\gamma\eta^9 - 2700N_BS^2Sc^2\gamma^2\eta^7 \\ &-3600N_BRdS^2Sc^2\gamma^2\eta^7 + 1440N_BS^2Sc\gamma^2\eta^7 \end{aligned}$$

$$+1920N_BRdS^2Sc\gamma^2\eta^7+360N_BM^2SSc\gamma^2\eta^7+\cdots)$$

$$F_3(\eta)=\frac{1}{21189168000(\gamma+1)^3}(-175175\gamma^3M^6\eta^9$$

$$+1261260\gamma^3M^6\eta^7-3405402\gamma^3M^6\eta^5+3727724\gamma^3M^6\eta^3$$

$$-1408407\gamma^3M^6\eta+57330\gamma^3M^4S\eta^{11}-2207205\gamma^3M^4S\eta^9$$

$$+14702688\gamma^3M^4S\eta^7-39981942\gamma^3M^4S\eta^5+44397990\gamma^3M^4S\eta^3$$

$$-16968861\gamma^3M^4S\eta+14700\gamma^3M^2S^2\eta^{13}+322959\gamma^3M^2S^2\eta^{11}+\cdots)$$

$$G_3(\eta)=\frac{1}{8072064000(4Rd+3)^3\gamma(\gamma+1)^2}(5457375Pr^3S^3\gamma^3\eta^{13}$$

$$-935550Pr^2S^3\gamma^3\eta^{13}-26880PrRd^2S^3\gamma^3\eta^{13}-15120PrS^3\gamma^3\eta^{13}$$

$$-1247400Pr^2RdS^3\gamma^3\eta^{13}-40320PrRdS^3\gamma^3\eta^{13}$$

$$+10914750Pr^3S^3\gamma^2\eta^{13}-935550Pr^2S^3\gamma^2\eta^{13}$$

$$-1247400Pr^2RdS^3\gamma^2\eta^{13}+5457375Pr^3S^3\gamma\eta^{13}+\cdots)$$

$$H_3(\eta)=\frac{1}{24216192000N_B(4Rd+3)^2\gamma(\gamma+1)^2}(9702000N_BRd^2S^3$$

$$Sc^3\gamma^3\eta^{13}+5457375N_BS^3Sc^3\gamma^3\eta^{13}+14553000N_BRdS^3Sc^3\gamma^3\eta^{13}$$

$$-1663200N_BRd^2S^3Sc^2\gamma^3\eta^{13}-935550N_BS^3Sc^2\gamma^3\eta^{13}$$

$$-2494800N_BRdS^3Sc^2\gamma^3\eta^{13}-26880N_BRd^2S^3Sc\gamma^3\eta^{13}$$

$$-15120N_BS^3Sc\gamma^3\eta^{13}-40320N_BRdS^3Sc\gamma^3\eta^{13}+\cdots)$$

3.2. Finite Difference Method. One of the simplest and well established numerical method prevailing today to solve non-linear differential equations with no exact solution is the FDM. In the current study, FDM is directly implemented on the non-linear ordinary differential equations obtained by adopting similarity transformations on the governing non-linear partial differential equations. The basic principle of this technique is to adopt Taylor's series expansion in discretising the derivatives of the variables. In order to compare the numerical values of coefficient of skin friction, and heat and mass transfer rates obtained by employing HPM, classical FDM is adopted to obtain the numerical values for the same.

4. Results and Discussion

A theoretical analysis on the influence of thermal radiation and viscous dissipation on the heat and mass transfer characteristics on the unsteady squeezing MHD flow of Casson fluid between parallel plates is presented in the current article. HPM is employed to determine the axial velocity and radial velocity fields, temperature distribution curves, and concentration profiles for different values of the pertaining physical parameters involved in the problem and are presented in Figs. (2 - 23). Tables (1 - 4) represent the numerical values of magnitude of skin friction coefficient, heat and mass transfer rates for various values of the physical parameters considered.Further, in order to compare the results obtained, Tables (1 - 4) facilitates HPM and FDM values obtained for different values of the physical parameters in accordance to the numerical values of magnitude of coefficient of skin friction, heat and mass transfer.

Figs. (2 - 5) graphically represent the impact of squeeze number S on the axial velocity $F(\eta)$, radial velocity $F'(\eta)$, temperature $G(\eta)$ and concentration $H(\eta)$ respectively. An increase in the squeeze number increases the shear rate which in turn increases the viscosity of the Casson fluid. Thus, the axial velocity of the Casson fluid flowing between parallel plates increase as a result of the increase in viscosity. Moreover, an increase in the squeeze number increases the fluid deformation, which leads to an increase in the velocity gradient within the fluid. Due to this higher velocity gradient, the fluid's axial velocity increases. Further, an increase in the squeeze number increases the heat generated within the fluid which is then transferred to the fluid, causing an increase in the temperature of the fluid. Thus, leading to an increase in the temporal profile. It is evident for the graphs that an increase in S increases $F(\eta)$, $G(\eta)$ and $H(\eta)$. The concentration of the Casson fluid flow between parallel increases with an increase in the squeeze number because an increase in the squeezing increases pressure on the fluid, causing the fluid to compress and become more dense. As a result of this compression the fluid concentration increases along the plates leading to a higher concentration profile. Whereas in the case of radial velocity, an increase in S results in decrease of $F'(\eta)$ in the first half and increases in the range $0.45 \leq \eta \leq 1$. A decrease in the radial velocity in the first half, with an increase in the squeeze number can be attributed to the increase in the shear stress at the walls. The fluid experiences a higher rate of deformation with an increase in the squeeze number which results in an increase in the shear stress at the plates. This increase in shear stress causes the fluid particle to stick more to the plates which reduces the radial velocity in the first half. However, an increase in the squeeze number results in a faster flow of fluid due to higher resistance at the plates resulting in an increase in the radial velocity in the second half.

Due to the induction of Lorentz force by the magnetic field, that act against the the flow of the fluid, a resistance is experienced by the fluid which slows down the fluid flow causing the axial velocity of the Casson fluid to retards with an increase in the magnetic parameter. Moreover, the magnetic parameter can also alter the viscosity of the Casson fluid which in turns effects the flow behaviour. Further, due to the induced Lorentz force, a secondary flow is generated. The so generated

secondary flow is perpendicular to the direction of the magnetic field applied which increases the mixing and thus is responsible for retardation in the temporal profile. Also as the Lorentz force effects the velocity and dynamic viscosity of the Casson fluid flow, the heat transfer characteristics is also affected by the a change in the magnetic parameter. Additionally, the induced magnetic field generates eddy current which further effects the temporal profile. Figs. (6 - 9) present graphically the effect of magnetic parameter M on the axial velocity $F(\eta)$, radial velocity $F'(\eta)$, temperature $G(\eta)$ and concentration $H(\eta)$ respectively . From the figures, it can be noted that an increase in M decreases the axial velocity and the temporal profile, whereas radial velocity and concentration profile increases irrespective of plates moving towards or away from each other. An increase in the magnetic parameter directly affects the distribution of the fluid particles leading to a change in the fluid viscosity. As the magnetic is increased, the strength of the magnetic field increases, which causes more fluid particles to align with the induced field. This alignment in turn affects the fluid's flow behaviour and thus increases the radial velocity. An increase in the magnetic parameter enhances the mixing of the fluid by inducing a secondary flow, as a result of which the concentration of fluid becomes uniform. Moreover, the magnetic field causes the fluid to deform, which further enhances the mixing of fluids leading to a more uniform concentration. As a result of this enhanced mixing and uniform concentration distribution, the concentration profile increases with an increase in the magnetic field.

Figs. (10 - 13) displays graphically the influence of Casson fluid parameter γ on the axial velocity $F(\eta)$, radial velocity $F'(\eta)$, temperature $G(\eta)$ and concentration $H(\eta)$ respectively. From the figures, it is clear that an increase in γ increases the axial velocity in the case of plates moving towards, whereas decreases as the plates move apart. In the case of plates moving towards each, an increase in the Casson fluid parameter increases the shear thinning behaviour of the Casson fluid. Due to a higher shear stress in a narrow gap between the two plates, the viscosity of the Casson fluid retards, resulting in an increased axial velocity. In the case of plates dilating, the shear thickening behaviour of the Casson fluid increases due to decrease in the shear rate. As a result an increase in the Casson fluid parameter results in a decrement of axial velocity as the plates dilate. The radial velocity increases with an increase in γ initially, whereas decreases in the second half as the plates move towards, whereas an opposite trend is observed in the case of plates moving apart. As the Casson fluid parameter increases, the fluid becomes more resistant to flow hence causing the radial velocity to decrease initially. However as the plates move closer, with increase in the Casson fluid parameter the shear rate within the fluid increases. This causes the fluid to thin and make the flow more easier. As a result, the radial velocity decreases in the second half. The temporal profile decreases with an increase in the Casson fluid parameter whereas the concentration profile increases in both cases, for plates approaching and receding from each other. This is because as the Casson fluid parameter increases, the viscosity of the fluid increases, which in turn is responsible for higher dissipation of heat. This heat dissipated thus reduces the temperature profile to retard with increase in the Casson fluid parameter. Further, the concentration profile of the Casson fluid flow increases with an increase in the Casson fluid parameter due to

higher viscosity and yield stress of Casson fluid. This implies that the fluid becomes more resistant to flow and require greater force to move it. As a result, the concentration of the fluid increases as the centre, which in turn creating a thicker layer of fluid that is more concentrated.

The repercussion of Prandtl number Pr on the temperature $G(\eta)$ and concentration $H(\eta)$ are respectively displayed in Figs. (14 & 15). The Prandtl number ia a dimensionless number that is used to characterise the ability of the fluid to conduct heat and diffuse momentum. An increase in the Prandtl number increases the thermal diffusivity of the fluid, which on turn increases the fluid's temperature at the plates. Thus, an increase in the Prandtl number must increase the temporal profile of the fluid. It is observed from the figures that an elevation in Pr elevates the temporal profile in both cases, for plates approaching and receding from each other. On the other hand, an increment in Pr results in decrement of the concentration profile in both the cases. This is because increase in Prandtl number increases the mass diffusivity of the fluid, which increases the concentration of the fluid in both cases, for plates approaching and receding from each other.

The impact of radiation parameter Rd on the temperature $G(\eta)$ and concentration $H(\eta)$ are respectively displayed in Figs. (16 & 17). From the figures, it is apparent that an increase in Rd decreases the temporal profile in both cases, for plates approaching and receding from each other, whereas concentration profile elevates. As the radiation parameter increases, the temperature profile retards as a result of radiation causes the fluid to lose the heat energy to the surrounding environment. Further, an increase in the radiation parameter increases the shear rate of the fluid which in turn increases the fluid concentration. The effect of Eckert number Ec on the temperature $G(\eta)$ and concentration $H(\eta)$ are respectively displayed in Figs. (18 & 19). The Eckert number is a dimensionless parameter which relates the kinetic energy of the fluid to its thermal energy. An increase in the Eckert number directly impacts the boundary layer thickness and other flow properties. Due to increase in the rate of heat transfer caused by increase in the velocity as an after affect of increase in Eckert number, the temporal profile of the Casson fluid flow increases. It is evident from the figures that an increase in Ec increases the temporal profile in both cases, for plates approaching and receding from each other.On the contrary, the concentration profile retards with an increment in the Eckert number. The reason for this is that as the Eckert number increases, the fluid's kinetic energy increases as a result of which a retardation is seen in the concentration profile.

The repercussion of various parameters such as Nusselt number N_T, Brownian motion constant N_B, Schmidt number Sc and chemical reaction parameter Kr on the concentration profiles are respectively discussed in Figs. (20 - 23). The Nusselt number quantifies how efficiently heat is transferred via convection. As the convective heat transfer rate increases, the composition of the fluid becomes more homogeneous. This homogeneity results in a decrease in the concentration profile of the fluid. Moreover, the Casson fluid model posits that the fluid exhibits a yield stress, which indicates that it flows only when a certain threshold of shear stress is reached. As the Nusselt number rises, the shear stress exerted on the fluid

also increases, prompting more of the fluid to flow and reducing the concentration gradient. It is apparent from the figure that an increase in Nusselt number and chemical reaction parameters decrease the concentration profile in both the cases. When a chemical reaction occurs, the fluid's effective viscosity decreases, resulting in slower fluid velocity near the plates and a reduction in the concentration profile. Besides, a higher chemical reaction parameter can alter the flow structure, leading to additional impact on the concentration profile. It is observed that increase in Brownian motion constant increases the concentration profile in the case of plates receding from each other, whereas an opposite trend in the case of plates moving towards. When the Brownian motion constant is high, it causes the solute molecules to move more randomly in the fluid. This results in faster mass transfer between the plates and a higher concentration of the solute near the plates. When the plates move towards each other, the distance between them decreases, which also contributes to the increased concentration profile. However, an opposite behaviour to that of the Brownian motion constant is displayed by the Schmidt number. When two plates move apart, the solute molecules in the fluid layer between them cannot diffuse across quickly enough to keep up with the flow of the fluid. This results in an increase in the concentration profile. This phenomenon is more noticeable when the solute's diffusion coefficient is lower compared to the momentum diffusivity of the fluid, which is the case at higher Schmidt numbers.

The data presented in Table (1) indicates the impact of squeeze number, magnetic parameter and Casson fluid parameter on the magnitude of skin friction coefficient at the upper plate. From the table it is evident that an increase in Squeeze number and magnetic parameter result in an increase in the magnitude of skin friction coefficient at the upper plate, whereas increase in Casson Fluid parameter decreases the magnitude of coefficient of skin friction. The effect of squeeze number, magnetic parameter and Casson fluid parameter on the heat and mass transfer rates are demonstrated numerically in Table (3). It is observed that an increase in the Casson fluid parameter reduces the rate of heat transfer at the lower plate, whereas increases at the upper plate. However, squeeze number shows an opposite behaviour. Moreover, an increment in the magnetic parameter reduced the heat transfer rate at both the plates. Further, an increase in the squeeze number increases the mass transfer rate at the lower plate, whereas reduces at the upper plate. However an opposite behaviour is displayed by radiation parameter.

The repression of Prandtl number, radiation parameter and Eckert number on the rate of heat and mass transfer are numerically presented in Table (2). From the table it is apparent that an increase in the Prandtl number and Eckert number increase the rate of heat transfer at the lower plate and decrease the rate of heat transfer at the upper plate for both plates moving towards and apart from each other. Whereas, an increase in radiation parameter increases the rate of heat transfer at the upper plate and decreases the rate of heat transfer at the lower plate. Further, in the case of plates moving towards, the rate of mass transfer increases with increase in the Prandtl number at both the plates, whereas radiation parameter shows an opposite trend. The mass transfer rate retards with

increase in the Eckert number at the upper plate, whereas retards at the lower plate in the case of plates moving towards. In the case of plates moving apart, increase in Prandtl number and Eckert number decrease the rate of mass transfer at the bottom plate, whereas increase at the upper. However, an increment in the radiation parameter increases the rate of mass transfer at both the plates for plates moving apart. The influence of Nusselt number, Brownian motion constant and Schmidt number are numerically depicted in Table (4). From the table it is observed that an increase in N_T and Sc decreases the mass transfer rate at the lower plate whereas elevates at the upper plate in the case of plates moving towards. However, Brownian motion constant shows an opposite trend. In the case of plates moving apart, an opposite behaviour to that of the plates moving towards is displayed.

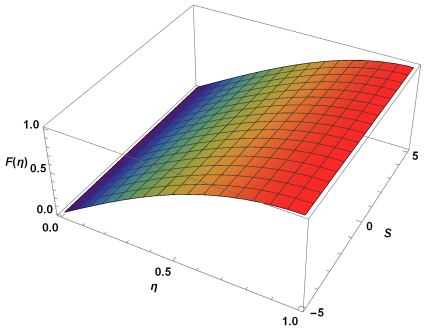

FIGURE 2. Impact of S on $F(\eta)$

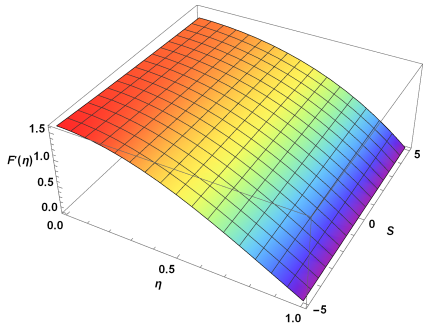

FIGURE 3. Impact of S on $F'(\eta)$

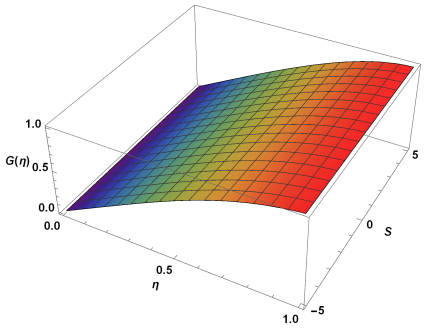

FIGURE 4. Impact of S on $G(\eta)$.

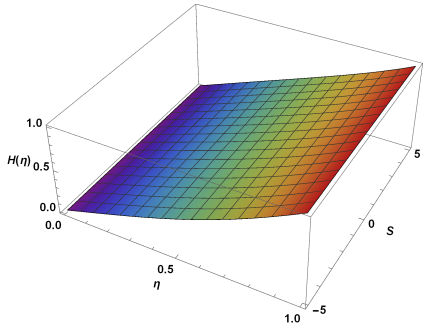

FIGURE 5. Impact of S on $H(\eta)$.

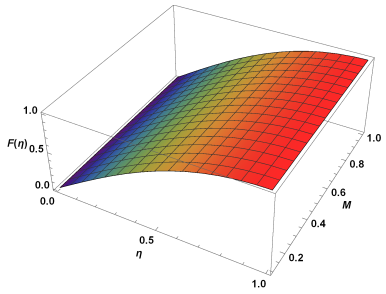

FIGURE 6. Impact of M on $F(\eta)$ for plates moving towards.

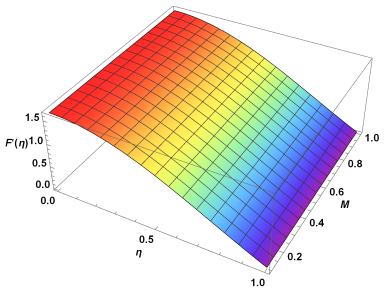

FIGURE 7. Impact of M on $F'(\eta)$ for plates moving towards.

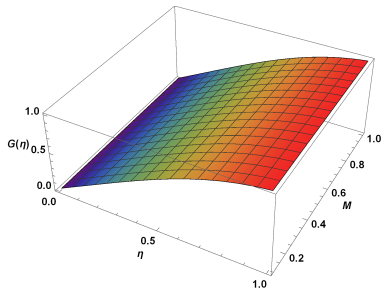

FIGURE 8. Impact of M on $G(\eta)$ for plates moving apart.

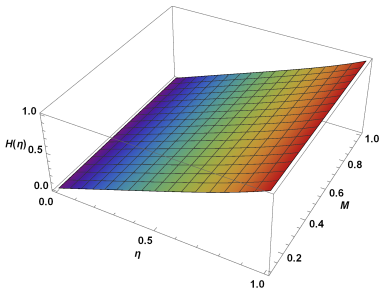

FIGURE 9. Impact of M on $H(\eta)$ for plates moving apart.

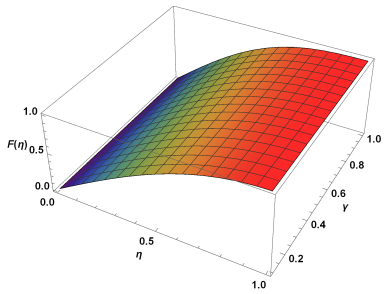

FIGURE 10. Impact of γ on $F(\eta)$ for plates moving towards.

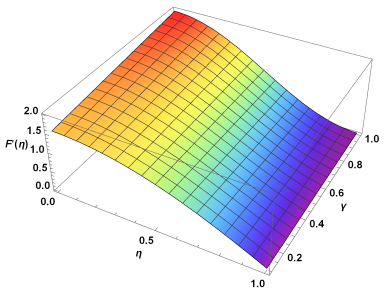

FIGURE 11. Impact of γ on $F'(\eta)$ for plates moving towards.

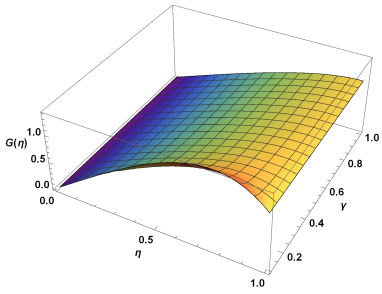

FIGURE 12. Impact of γ on $G(\eta)$ for plates moving apart.

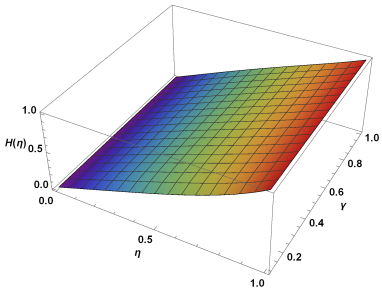

FIGURE 13. Impact of γ on $H(\eta)$ for plates moving apart.

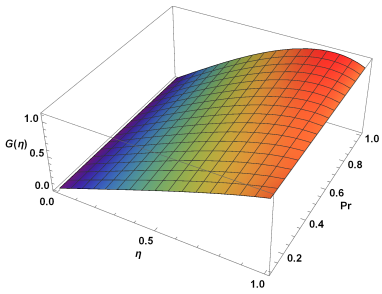

FIGURE 14. Impact of Pr on $G(\eta)$ for plates moving apart.

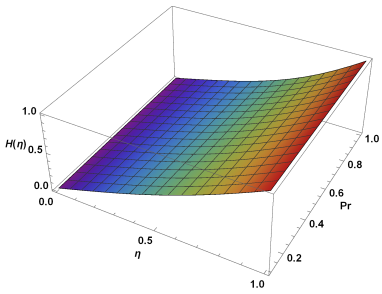

FIGURE 15. Impact of Pr on $H(\eta)$ for plates moving towards.

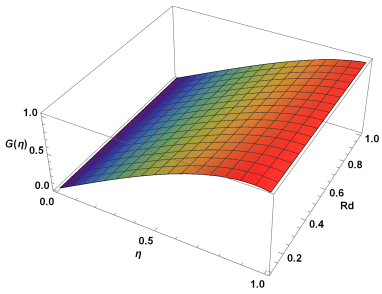

FIGURE 16. Impact of Rd on $G(\eta)$ for plates moving apart.

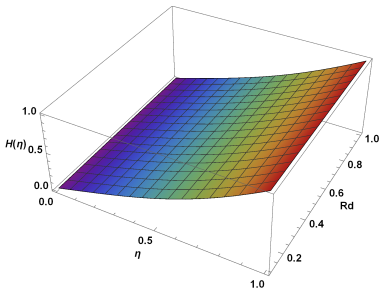

FIGURE 17. Impact of Rd on $H(\eta)$ for plates moving towards.

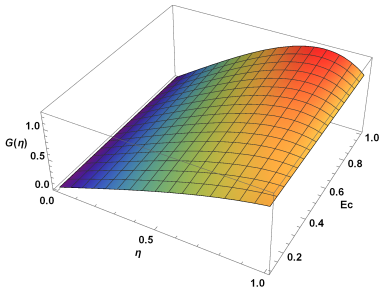

FIGURE 18. Impact of Ec on $G(\eta)$ for plates moving apart.

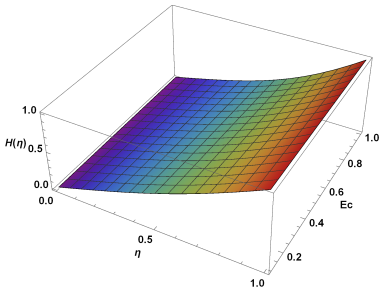

FIGURE 19. Impact of Ec on $H(\eta)$ for plates moving towards.

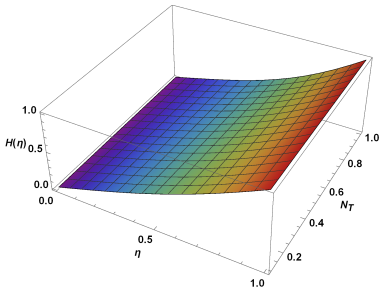

FIGURE 20. Impact of N_T on $H(\eta)$ for plates moving towards.

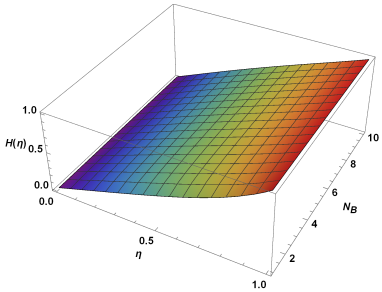

FIGURE 21. Impact of N_B on $H(\eta)$ for plates moving apart.

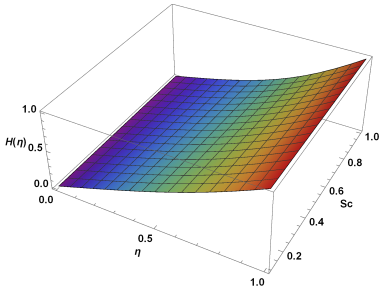

FIGURE 22. Impact of Sc on $H(\eta)$ for plates moving towards.

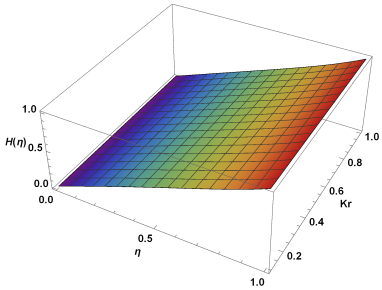

FIGURE 23. Impact of Kr on $H(\eta)$ for plates moving apart.

TABLE 1. Skin friction coefficient for different values of S, M and γ.

		$\left(1+\frac{1}{\gamma}\right)F''(1)$					
M	γ	$S=-5$		$S=0$		$S=5$	
		HPM	FDM	HPM	FDM	HPM	FDM
0.1	0.3	-8.73819	-8.73819	-13.002	-13.0008	-16.148	-16.1442
	0.5	-4.27253	-4.27328	-9.002	-9.00389	-12.0138	-11.995
0.3	0.3	-8.74656	-8.75808	-13.018	-13.0173	-16.1609	-16.1640
	0.5	-4.28276	-4.27635	-9.01798	-9.02276	-12.026	-12.009

TABLE 2. Heat and mass transfer rates for $M=0.2$, $\gamma=0.5$, $N_T=0.1$, $N_B=10$, $Sc=0.3$ and $Kr=0.5$.

Ec	Rd	$G'(0)$		$G'(1)$		$H'(0)$		$H'(1)$	
		HPM	FDM	HPM	FDM	HPM	FDM	HPM	FDM
		$S=-5$							
		$Pr=0.1$							
0.1	0.3	1.00077	1.00103	0.985824	0.985042	0.863142	0.862472	1.17771	1.17783
	0.5	1.00066	1.00082	0.988091	0.987383	0.863141	0.862473	1.17768	1.17781
0.3	0.3	1.05834	1.06001	0.897334	0.89543	0.862991	0.861917	1.17859	1.17874
	0.5	1.04909	1.05045	0.91382	0.912175	0.863043	0.862006	1.17842	1.17857
		$Pr=0.3$							
0.1	0.3	1.0018	1.00318	0.957526	0.955753	0.863152	0.86246	1.17798	1.17812
	0.5	1.00162	1.00274	0.964309	0.962785	0.863149	0.862462	1.17791	1.17805
0.3	0.3	1.17124	1.17661	0.823483	0.684076	0.861599	0.86083	1.18064	1.18086
	0.5	1.14461	1.14913	0.851972	0.735137	0.861838	0.861086	1.18014	1.18035
		$S=5$							
		$Pr=0.1$							
0.1	0.3	1.02951	1.02882	0.924238	0.924268	1.04638	1.04578	0.966205	0.966084
	0.5	1.02476	1.02413	0.936337	0.936307	1.04642	1.04582	0.966088	0.965966
0.3	0.3	1.05416	1.05291	0.813742	0.844003	1.04614	1.04562	0.967285	0.967171
	0.5	1.04544	1.04434	0.843507	0.814399	1.04623	1.04553	0.966995	0.96688
		$Pr=0.3$							
0.1	0.3	1.05934	1.08817	0.773773	0.774581	1.04579	1.04518	1.05094	0.967553
	0.5	1.04976	1.07381	0.809753	0.810369	1.04594	1.04532	1.05071	0.967202
0.3	0.3	1.10908	1.16182	0.442886	0.445658	1.04508	1.0443	1.05381	0.970807
	0.5	1.09142	1.13539	0.531682	0.533932	1.04534	1.0477	1.05312	0.964936

TABLE 3. Heat and mass transfer rates for $Pr = 0.3$, $Rd = 0.5$, $Ec = 0.3$, $N_T = 0.1$, $N_B = 10$, $Sc = 0.3$ and $Kr = 0.5$.

M	γ	$G'(0)$		$G'(1)$		$H'(0)$		$H'(1)$	
		HPM	FDM	HPM	FDM	HPM	FDM	HPM	FDM
		$S = -5$							
0.1	0.3	1.18455	1.18489	0.579744	0.578782	0.872712	0.872373	1.17158	1.17130
	0.5	1.14484	1.14922	0.739659	0.734972	0.861771	0.861014	1.1802	1.18041
0.3	0.3	1.18412	1.18463	0.579602	0.578711	0.872811	0.872473	1.1715	1.17121
	0.5	1.14423	1.14868	0.739595	0.735158	0.86195	0.861205	1.18004	1.18024
		$S = 5$							
0.1	0.3	1.18988	1.18895	0.369828	0.370983	1.04864	1.0482	0.968578	0.968264
	0.5	1.13797	1.13543	0.531772	0.534007	1.04535	1.04501	0.970015	0.970168
0.3	0.3	1.18975	1.18881	0.369604	0.370768	1.04859	1.04815	0.968614	0.968302
	0.5	1.13789	1.13531	0.531532	0.533801	1.04531	1.04466	0.970057	0.969966

TABLE 4. Mass transfer rate for $M = 0.2$, $\gamma = 0.5$, $Pr = 0.3$, $Rd = 0.5$, $Ec = 0.3$ and $Kr = 0.5$.

N_T	N_B	Sc	$H'(0)$		$H'(1)$	
			HPM	FDM	HPM	FDM
			$S = -5$			
0.1	1	0.1	0.939327	0.937978	1.08436	1.08524
		0.5	0.766813	0.765389	1.32378	1.32529
	5	0.1	0.950195	0.949628	1.06384	1.06396
		0.5	0.776774	0.776022	1.30319	1.30394
0.3	1	0.1	0.912157	0.908706	1.13568	1.13821
		0.5	0.741911	0.738804	1.37527	1.37866
	5	0.1	0.944761	0.943782	1.0741	1.07457
		0.5	0.771794	0.770706	1.31349	1.31462
			$S = 5$			
0.1	1	0.1	1.00245	1.0017	1.03409	1.03427
		0.5	1.06401	1.06307	0.989926	0.99051
	5	0.1	1.01298	1.0126	0.997229	0.997158
		0.5	1.07474	1.07413	0.953821	0.954097
0.3	1	0.1	0.976116	0.974442	1.12626	1.12705
		0.5	1.03718	1.03543	1.08019	1.08154
	5	0.1	1.00772	1.00715	1.01566	1.01571
		0.5	1.06938	1.0686	0.971874	0.972303

5. Conclusion

The current study aims to theoretically examine the impact of thermal radiation on the heat and mass transfer characteristics on the flow of MHD Casson fluid between a pair of parallel plates. The repercussion of various physical parameters on the flow of MHD Casson Fluid in the presence of thermal radiation are analysed by employing HPM. The following conclusions are extracted from this study.

- The magnetic parameter shows positive impact on the axial velocity and the concentration profile.
- The temporal distribution curve retards as the radiation parameter increases, whereas the concentration distribution curve elevates.
- The temporal profile elevates with a hike in Eckert number, whereas the concentration field retards.
- As the plates move closer to each other, the concentration distribution curve retards with an increment in the Nusselt number, whereas elevates with an increase in the Brownian motion constant.
- As the plates dilate, the concentration distribution profile retards with an elevation in the chemical reaction parameter, whereas elevates with increase in Schmidt number.

Acknowledgment. The authors are thankful to Manipal Academy of Higher Education (MAHE), Manipal for their support.

Nomenclature

Parameter	Notation	Formula
Squeeze number	S	$S = \frac{\alpha d^2}{2\nu}$
Magnetic parameter	M	$M = B_0 a \sqrt{\frac{\sigma(1-\alpha t)}{\mu}}$
Prandtl number	Pr	$Pr = \frac{\mu C_p}{k}$
Radiation parameter	Rd	$Rd = \frac{4\sigma^* T_1^3}{k^* k}$
Eckert number	Ec	$Ec = \frac{1}{C_p(T_2 - T_1)} \left(\frac{\alpha x}{2(1-\alpha t)}\right)^2$
Nusselt number	N_T	$N_T = \frac{D_T(T_2 - T_1)}{\nu T_1}$
Brownian motion constant	N_B	$N_B = \frac{D_B(C_2 - C_1)}{\nu}$
Schmidt number	Sc	$Sc = \frac{\nu}{D_B}$
Chemical reaction parameter	Kr	$Kr = \frac{k_1 a^2(1-\alpha t)}{\nu}$

References

1. Wang, C. Y.: The squeezing of a fluid between two plates, in: *Journal of Applied Mechanics*, **43(4)** (1976) 579–583.
2. Gupta, P. S., Gupta, A. S.: Squeezing flow between parallel plates, in: *Wear*, **45(2)** (1977) 177–185.
3. Singh, P., Radhakrishnan, V., Narayan, K. A.: Squeezing flow between parallel plates, in: *Ingenieur-Archiv*, **60** (1990) 274–281.

4. Ghori, Q. K., Ahmed, M., Siddiqui, A. M.: Application of Homotopy Perturbation Method to Squeezing Flow of a Newtonian Fluid, in: *International Journal of Nonlinear Sciences and Numerical Simulation*, **8(2)** (2007) 179–184.
5. Bujurke, N. M., Achar, P. K., Pai, N. P.: Computer extended series for squeezing flow between plates, in: *Fluid Dynamics Research*, **16(2-3)** (1995) 173–187.
6. Petrov, A. G., Kharlamova, I. S.: The solutions of Navier–Stokes equations in squeezing flow between parallel plates, in: *European Journal of Mechanics - B/Fluids* **48** (2014) 40–48.
7. Siddiqui, A. M., Irum, S., Ansari, A. R.: Unsteady squeezing flow of a viscous MHD fluid between parallel plates, a solution using the homotopy perturbation method, in: *Mathematical Modelling and Analysis* **13(4)** (2008) 565–576.
8. Sweet, E., Vajravelu, K., Gorder, R. A. V., Pop, I.: Analytical solution for the unsteady MHD flow of a viscous fluid between moving parallel plates, in: *Communications in Nonlinear Science and Numerical Simulation* **16(1)** (2011) 266–273.
9. Hatami, M., Hosseinzadeh, K., Domairry, G., Behnamfar, M. T.: Numerical study of MHD two-phase Couette flow analysis for fluid-particle suspension between moving parallel plates, in: *Journal of the Taiwan Institute of Chemical Engineers* **45(5)** (2014) 2238–2245.
10. Baag, S., Acharya, M. R., Dash, G. C., Mishra, S. R.: MHD flow of a visco-elastic fluid through a porous medium between infinite parallel plates with time dependent suction, in: *Journal of Hydrodynamics* **27(5)** (2015) 738–747.
11. Afikuzzaman, M., Alam, M. M.: MHD casson fluid flow through a parallel plate, in: *Science & Technology Asia* **21(1)** (2016) 59–70.
12. Hussain, Z., Zuev, S., Kabobel, A., Sultan, M. A., Shahzad, M.: MHD instability of two fluids between parallel plates, in: *Applied Nanoscience* **10** (2020) 5211–5218.
13. Duwairi, H. M., Tashtoush, B., Damseh, R. A.: On heat transfer effects of a viscous fluid squeezed and extruded between two parallel plates, in: *Heat and Mass Transfer* **41(2)** (2004) 112–117.
14. Dogonchi, A. S., Divsalar, K., Ganji, D. D.: Flow and heat transfer of MHD nanofluid between parallel plates in the presence of thermal radiation, in: *Computer Methods in Applied Mechanics and Engineering*, **310** (2016) 58–76.
15. Kumar, M. S., Sandeep, N., Kumar, B. R.: Effect of nonlinear thermal radition on unsteady MHD flow between parallel plate, in: *Global Journal of Pure and Applied Mathematics*, **12(1)** (2016) 60–65.
16. Raptis, A., Perdikis, C., Takhar, H. S.: Effect of thermal radiation on MHD flow, in: *Applied Mathematics and Computation*, **153(3)** (2004) 645–649.
17. Sheikholeslami, M., Ganji, D. D., Javed, M. Y., Ellahi, R.: Effect of thermal radiation on magnetohydrodynamics nanofluid flow and heat transfer by means of two phase model, in: *Journal of magnetism and Magnetic materials*, **374** (2006) 36–43.
18. Harfouf, E. A., Wakif, A., Mounir, S. H.: Heat transfer analysis on squeezing unsteady MHD nanofluid flow between two parallel plates considering thermal radiation, magnetic and viscous dissipations effects a solution by using Homotopy Perturbation method, in: *Sensor Letters*, **18(2)** (2020) 113–121.
19. Mustafa, M., Hayat, T., Obaidat, S.: On heat and mass transfer in the unsteady squeezing flow between parallel plates, in: *Meccanica*, **47** (2012) 1581-–1589.
20. Saif, A. S. A., Harfash, A.: Perturbation-iteration algorithm for solving heat and mass transfer in the unsteady squeezing flow between parallel plates, in: *Journal of Applied and Computational Mechanics*, **5(4)** (2019) 804–815.
21. Singh, K., Rawat, S. K., Kumar, M.: Heat and mass transfer on squeezing unsteady MHD nanofluid flow between parallel plates with slip velocity effect, in: *Journal of Nanoscience*, **2016** (2016) 1–11.
22. Alreshidi, N. A., Shah, Z., Dawar, A., Kumam, P., Shutaywi, M., Watthayu, W.: Brownian motion and thermophoresis effects on MHD three dimensional nanofluid flow with slip conditions and Joule dissipation due to porous rotating disk, in: *Molecules*, **25(3)** (2019) 1–20.
23. Bejawada, S. G., Reddy, Y. D., Rao, V. S., Khan, Z. H.: Thermal radiation and Joule heating effects on magnetohydrodynamic Casson nanofluid flow in the presence of chemical reaction

through a non-linear inclined porous stretching sheet, in: *Journal of Naval Architecture and Marine Engineering*, **17(2)** (2020) 143–164.
24. Mohamed, R. A., Rida, S. Z., Arafa, A. A. M., Mubarak, M. S.: Heat and Mass Transfer in an Unsteady Magnetohydrodynamics Al2O3–Water Nanofluid Squeezed Between Two Parallel Radiating Plates Embedded in Porous Media With Chemical Reaction, in: *Journal of Heat Transfer*, **142(1)** (2020) 012401.
25. Bejawada, S. G., Reddy, Y. D., Jamshed, W., Nisar, K. S., Alharbi, A. N., Chouikh, R.: Radiation effect on MHD Casson fluid flow over an inclined non-linear surface with chemical reaction in a Forchheimer porous medium, in: *Alexandria Engineering Journal*, **61** (2022) 8207—8220.
26. Alqarni, M. M., Bilal, M., Allogmany, R., Eldin, E. T., Ghoneim, M. E., Yassen, M. F.: Mathematical analysis of casson fluid flow with energy and mass transfer under the influence of activation energy from a non-coaxially spinning disc, in: *Frontiers in Energy Research*, **10** (2022) 986284.
27. Pai, N. P., Devaki, B., Pareekshith, Sampath, K. V. S., Vasanth, K. R.: Radiation effect on MHD Casson fluid flow between parallel plates of different permeability, in: Global and Stochastic Analysis **10(2)** (2023) 135–149.
28. Khan, U., Ahmed, N., Khan, S. I., Bano, S., Din, S. T. M.: Heat transfer analysis for squeezing flow of a Casson fluid between parallel plates, in: *World Journal of Modelling and Simulation*, **10(4)** (2014) 308–319.
29. Khan, U., Khan, S. I., Ahmed, N., Bano, S., Din, S. T. M.,: Heat transfer analysis for squeezing flow of a Casson fluid between parallel plates, in: *Ain Shams Engineering Journal*, **7(1)** (2016) 497–504.
30. Sampath, K. V. S., Pai, N. P.: A study on magnetic effect on flow between two plates with suction or injection with special reference to Casson fluid, in: *Frontiers in Heat and Mass Transfer*, **12(23)** (2019) 1–9.
31. Noor, N. A. M., Shafie, S., Admon, M. A.: MHD squeezing flow of Casson nanofluid with chemical reaction, thermal radiation and heat generation/absorption, in: *Journal of Advanced Research in Fluid Mechanics and Thermal Sciences*, **68(2)** (2020) 94–111.
32. Obalalu, A. M.: Heat and mass transfer in an unsteady squeezed Casson fluid flow with novel thermophysical properties: Analytical and numerical solution, in: *Heat Transfer*, **50(8)** (2021) 7988–8011.
33. Sampath, K. V. S., Pai, N. P., Devaki, B.: Heat transfer analysis of MHD Casson fluid flow between two porous plates with different permeability, in: *Frontiers in Heat and Mass Transfer*, **20(30)** (2023) 1–13.
34. He, J. H.: Homotopy perturbation technique, in: *Computer Methods in Applied Mechanics and Engineering*, **178(3)** (1999) 257–262.
35. He, J. H.: A coupling method of a homotopy technique and a perturbation technique for non-linear problems, in: *International Journal of Non-Linear Mechanics*, **35(1)** (2000) 37–43.
36. He, J. H.: Homotopy perturbation method: a new nonlinear analytical technique, in: *Applied Mathematics and Computation*, **135(1)** (2003) 73-79.
37. Babolian, E., Azizi, A. and Saeidian, J.: Some notes on using the homotopy perturbation method for solving time-dependent differential equations, in: Mathematical and computer modelling, **50(1-2)** (2009) 213–224.
38. Gupta, S., Kumar, D., Singh, J.: Application of he's homotopy perturbation method for solving non-linear wave-like equations with variable coefficients, in: *International Journal of Advances in Applied Mathematics and Mechanics*, **1(2)** (2009) 65–79.
39. Sampath, K. V. S., Pai, N. P., Jacub, K.: A semi-numerical approach to unsteady squeezing flow of casson fluid between two parallel plates, in: Malaysian Journal of Mathematical Sciences, **12(1)** (2018) 35–47.
40. Akter, M. T., Chowdhury, M. A. M.: Homotopy Perturbation Method for Solving Highly Non-linear Reaction-Diffusion-Convection Problem, in: *American Journal of Mathematics and Statistics*, **9(3)** (2019) 136–141.

41. Sachdev, P. L., Bujurke, N. M., Pai, N. P.: Dirichlet series solution of equations arising in boundary layer theory, in: *Mathematical and Computer Modelling*, **32(9)** (2000) 971–980.
42. Ali, M. M., Chen, T.S., Armaly, B.F.: Natural Convection-Radiation Interaction in Boundary-Layer Flow over Horizontal Surfaces, in: *AIAA JOURNAL*, **22(12)** (1984) 1797–1803.

Pareekshith G. Bhat: Department of Mathematics, Manipal Institute of Technology, Manipal Academy of Higher Education, Manipal, Karnataka 576104, India
Email address: pareekshith.mitmpl2022@learner.manipal.edu

Nityanand P. Pai: Department of Mathematics, Manipal Institute of Technology, Manipal Academy of Higher Education, Manipal, Karnataka 576104, India
Email address: nppaimit@yahoo.co.in

Devaki B.: Department of Mathematics, Manipal Institute of Technology, Manipal Academy of Higher Education, Manipal, Karnataka 576104, India
Email address: devakibadekkila@gmail.com

Sampath Kumar V. S.: Department of Mathematics, Manipal Institute of Technology, Manipal Academy of Higher Education, Manipal, Karnataka 576104, India
Email address: sampath.kvs@manipal.edu * Corresponding author